Available online at www.sciencedirect.com
ScienceDirect
Solar Energy 85 (2011) 2349–2359
SOLAR ENERGY
www.elsevier.com/locate/solener

An improved modeling method to determine the model parameters of photovoltaic (PV) modules using differential evolution (DE)

Kashif Ishaque, Zainal Salam *

Faculty of Electrical Engineering, Universiti Teknologi Malaysia, UTM 81310, Skudai, Johor Bahru, Malaysia

Received 16 April 2011; accepted 23 June 2011
Available online 23 July 2011

Communicated by: Associate Editor Takhir Razykov

Abstract

To accurately model the PV module, it is crucial to include the effects of irradiance and temperature when computing the value of the model parameters. Considering the importance of this issue, this paper proposes an improved modeling approach using differential evolution (DE) method. Unlike other PV modeling techniques, this approach enables the computation of model parameters at any irradiance and temperature point using only the information provided by the manufacturer's data sheet. The key to this improvement is the ability of DE to simultaneously compute all the model parameters at different irradiance and temperature. To validate the accuracy of the proposed model, three PV modules of different types (multi-crystalline, mono-crystalline and thin-film) are tested. The performance of the model is evaluated against the popular single diode model with series resistance R_s. It is found that the proposed model gives superior results for any irradiance and temperature variations. The modeling method is useful for PV simulator developers who require comprehensive and accurate model for the PV module.

Keywords: Differential evolution (DE); Mono-crystalline; Multi-crystalline; Photovoltaic (PV) module; Thin-film

1. Introduction

The modeling of PV module primarily involves the approximation of the non-linear I–V curves. Over the years, the circuit based approach has been widely used to characterize the PV module. The simplest model is the current source in parallel to a diode (Yun Tiam et al., 2004; Kajihara and Harakawa, 2005). It involves the determination of three model parameters, namely photo-current (I_{PV}), diode saturation current (I_o) and ideality factor (a). An improved version includes an additional series resistance (R_s) to the circuit (Khouzam et al., 1994; Walker, 2001; Weidong et al., 2004; Chenni et al., 2007; Matagne et al., 2007). This is known as R_s-model. Although this model is more accurate, it exhibits serious deficiencies when subjected to high temperature variations because it does not account for the open circuit voltage coefficient, K_V (Walker, 2001). Furthermore, it suites well for crystalline module (i.e. mono and multi crystalline), but exhibits considerable inaccuracy when applied to the thin-film technology (Ishaque et al., 2011). A further modification which includes a resistance, R_p in parallel to the diode was suggested by various authors (Chegaar et al., 2001; Shengyi and Dougal, 2002; Sera et al., 2007; Villalva et al., 2009). This model known in literature as R_p-model offers a good compromise between simplicity and accuracy and has been applied widely (Carrero et al., 2007). With the inclusion of R_p, however, the number of parameters is increased to five namely I_{PV}, I_o, a, R_s and R_p.

Due to the transcendental nature of the current equation for PV module, significant computation effort is required to obtain all the five model parameters. Out of these, only I_{PV}

* Corresponding author. Tel.: +60 75536187; fax: +60 75566272.
E-mail addresses: kashif@fkegraduate.utm.my (K. Ishaque), zainals@fke.utm.my (Z. Salam).

0038-092X/$ - see front matter © 2011 Elsevier Ltd. All rights reserved.
doi:10.1016/j.solener.2011.06.025

and I_o can be calculated analytically (Villalva et al., 2009). The remaining parameters, i.e. a, R_s and R_p have to be determined numerically. These normally involve iterative process using numerical methods such as Newton Raphson (Villalva et al., 2009). Consequently, a, R_s and R_p cannot be computed simultaneously along with I_{PV} and I_o for a particular environmental condition i.e. temperature and irradiance. For instance, in (Walker, 2001), the value of R_s can be obtained analytically but the value of a has to be kept constant while R_p is assumed to be infinity. In (Matagne et al., 2007; Weidong et al., 2004) an iterative method is used to estimate the values of a and R_s. However, the effect of R_p was not considered in the computation. In (Villalva et al., 2009), the value of R_s and R_p are iterated simultaneously but a constant value of a has to be used.

Since the physical behavior of PV module are strongly influenced by irradiance and temperature, it is imperative to compute all the model parameters simultaneously. Failing to do so, as the approaches mentioned above demonstrated, causes certain degree of degradation in accuracy. Recently several works have been carried out to resolve this issue using artificial intelligence (AI) techniques such as fuzzy logic (FL) (Elshatter et al., 1997) and artificial neural network (ANN) (Balzani and Reatti, 2005; Karatepe et al., 2006; Mellit et al., 2007; Almonacid et al., 2009, 2010; Syafaruddin et al., 2010). Despite the promising results, these techniques require extensive computation. For example, FL has to deal with fuzzification, rule base storage, inference mechanism and defuzzification operations. For ANN, large amount of data for training could be a major source of constraint. These drawbacks would be crucial when integrating the model parameters algorithms to the PV simulator.

Evolutionary algorithms (EA) techniques have gained much attention due to its ability to handle nonlinear functions without requiring derivatives information. It is a stochastic optimization method that appears to be very efficient in optimizing real-valued multi-modal objective functions. Various EA techniques such as genetic algorithm (GA) (Jervase et al., 2001; Moldovan et al., 2009), particle swarm optimization (PSO) (Ye et al., 2009) are employed for computation of PV cell parameters. However, these methods require extensive $I-V$ data sets as an input. Moreover, several computational difficulties, namely premature convergence, low speed and large number of iterations are observed (Zwe-Lee, 2004; Ji et al., 2006). Recently, another type of EA technique known as differential evolution (DE) was introduced (Storn and Price, 1997). It has three distinct advantages (1) able to accurately locate the global optimum point regardless of the initial condition (2) has rapid convergence (3) utilizes few control parameters.

Considering the many advantages of DE, this work proposes a method to simultaneously compute the values of a, R_s, and R_p, for different environmental condition. Unlike previous methods, this approach enables the computation to be done at any irradiance and temperature point (other than STC) using only the information provided by the manufacturer's data sheet. Furthermore, it eliminates the need for experimental $I-V$ data sets. As a result, the computation of the model parameters becomes simpler and more flexible. Furthermore, the speed of computation makes the integration of DE into a PV simulator to be more efficient.

The remainder of this paper is organized in the following way. Section 2 describes the details of the circuit model for PV module which is the basis for the computation of the parameters. Section 3 explains the background of DE theory, while, Section 4 describes how this technique is used to compute the model parameters. Section 5 shows the validation of the proposed algorithm to the experimental $I-V$ data set. The accurateness of the model is verified by applying the model to three PV modules of different types (mono-crystalline, multi-crystalline, and thin-film). The performance of the model is evaluated against a popular R_s-model. Finally, Section 6 draws the conclusions of this paper.

2. Circuits models for PV module

2.1. Ideal PV model

An ideal PV cell consists of a single diode connected in parallel with a light generated current source (I_{PV}) is shown in Fig. 1. Its output current can be written as

$$I = I_{PV} - I_o\left[\exp\left(\frac{V}{aV_T}\right) - 1\right] \quad (1)$$

where I_{PV} is the current generated by the incidence of light, I_o is the reverse saturation current, $V_T(=N_s\,kT/q)$ is the thermal voltage of the PV module having N_s cells connected in series, q is the electron charge ($1.60217646 \times 10^{-19}$ C), k is the Boltzmann constant ($1.3806503 \times 10^{-23}$ J/K), T is the temperature of the p–n junction in K, and a is the diode ideality factor.

2.2. PV model with series resistance, R_s

The R_s-model, depicted in Fig. 1b, is achieved with inclusion of series resistance R_s. The output current in Fig. 2 can be derived as

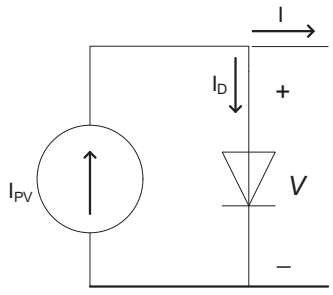

Fig. 1. Ideal PV circuit model.

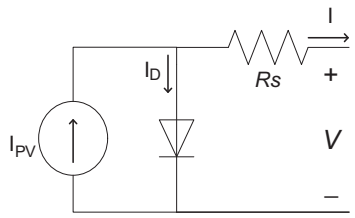

Fig. 2. PV circuit model with series resistance, R_s.

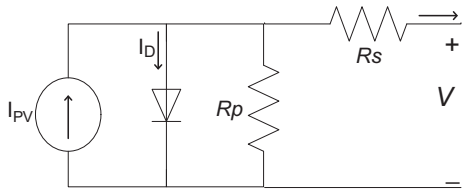

Fig. 3. PV circuit model with series and parallel resistance, R_s and R_p.

$$I = I_{PV} - I_0\left[\exp\left(\frac{V + IR_S}{aV_T}\right) - 1\right] \tag{2}$$

2.3. PV model with series and parallel resistance, R_s and R_p

Eq. (2) does not adequately represent the behavior of the cell when subjected to environmental variations, especially at low voltage. A more practical model can be seen in Fig. 3, where R_s and R_p represents the equivalent series and parallel resistances, respectively. An output current equation using this model can be written as:

$$I = I_{PV} - I_0\left[\exp\left(\frac{V + IR_S}{aV_T}\right) - 1\right] - \left(\frac{V + IR_S}{Rp}\right) \tag{3}$$

This model yields more accurate result than the R_s-model, but at the expense of longer computational time.

A modification of this model was proposed by several authors (Gow and Manning, 1999; Nishioka et al., 2007; Kassis and Saad, 2010; Ishaque et al., 2011) by adding an extra diode. This additional diode represents the recombination effects of the charge carriers. In general, the two diode model is more accurate but the computational time is much longer. For simplicity, the single diode model of Fig. 3 is used in this paper. This model offers a good compromise between simplicity and accuracy (Carrero et al., 2007), and has been utilized by numerous authors.

In most cases, the datasheets of PV module give the following information: the nominal short-circuit current $I_{sc,n}$, the nominal open-circuit voltage $V_{oc,n}$, voltage at the MPP V_{mp}, current at the MPP I_{mp}, temperature coefficient of open circuit voltage K_V, temperature coefficient of short circuit current K_I, and the maximum peak output power P_{mp}. This information is always provided with reference to the nominal conditions or standard test conditions (STC) of temperature and solar irradiation.

3. Differential evolution (DE)

Differential evolution (DE) was first introduced in (Storn and Price, 1997). The optimization procedure is similar to GA, but unlike GA, which relies on crossover, DE primarily utilizes mutation operation (i.e. difference vector) as a search and selection mechanism to direct the search toward the prospective regions in the search space. Like other EA family, DE relies on initial random population generation, which is then improved using selection, mutation, and crossover. The process is repeated through generations until the stopping condition is reached – usually a satisfactory good fitness value or a predefined maximum number of generations $G_{\max}$.

Like the other evolutionary algorithms, DE also works on a population, P_G, of candidate solutions. These candidate solutions are known as the individuals of the population. In particular, DE creates a population of NP D dimensional real-valued parameter vectors $X_{i,G}$ as:

$$P_{X,G} = (X_{i,G})\ i = 1, 2, \ldots, NP,\ G = 0, 1, \ldots, G_{\max} \tag{4}$$

$$X_{i,G} = (X_{j,i,G})\ j = 1, 2, \ldots, D \tag{5}$$

The index, $G = 0, 1, \ldots, G_{\max}$, indicates the generation to which a vector belongs. Additionally, each vector has a population index, i, from 1 to Np. Parameters within vectors are indexed with j, from 1 to D. The DE process involves following stages:

3.1. Initialization

In order to begin the optimization process, an initial population of NP D dimensional real-valued parameter vectors $X_{i\ ,G} = [X_{1,i,G}, X_{2,i,G}, \ldots, X_{j,i,G}, \ldots, X_{D,i,G}]$ is created. Each vector forms a candidate solution to the multi-dimensional optimization problem. Initial parameter values are usually randomly selected uniformly in the interval $[X_L, X_H]$, where $X_L = [X_{1,L}, X_{2,L}, \ldots, X_{D,L}]$ and $X_H = [X_{1,H}, X_{2,H}, \ldots, X_{D,H}]$ are the lower and upper bound of the search space, respectively.

$$X_{j,i,0} = X_L + rand[0, 1](X_H - X_L) \tag{6}$$

Fig. 4a explains the initialization procedure of DE. For simplicity, a 2-dimensional parameter space is shown here.

3.2. Mutation

Mutation is a perturbation or change with a random element. In literature, a parent vector from the current generation is known as *target* vector, a mutant vector achieved through the differential mutation operation is called a *donor* vector and finally an offspring formed by recombining the donor with the target vector is called *trial* vector. For a given parameter vector $X_{i,G}$, three vectors ($X_{r1,G}$, $X_{r2,G}$, $X_{r3,G}$) are randomly selected in the range [1, NP], such that the indices i, r_1, r_2 and r_3 are distinct. A donor

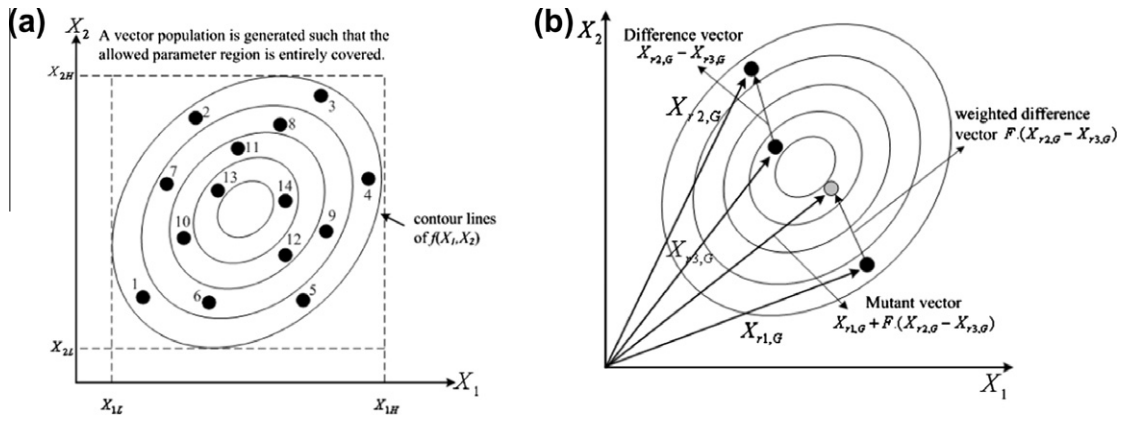

Fig. 4. (a) Initialization of DE. (b) Mutation process of DE.

vector $V_{i,G}$ is created by adding the weighted difference between the two vectors to the third (base) vector as:

$$V_{i,G} = X_{r1,G} + F(X_{r2,G} - X_{r3,G}) \tag{7}$$

where F is a mutation scaling factor, which is typically chosen from the range [0, 1]. Fig. 4b illustrates the process on a 2-D parameter space (showing constant cost contours of an arbitrary fitness function).

3.3. Crossover

The donor vector $V_{i,G+1}$ and the target vector $X_{i,G}$ are mixed to yield the trial vector

$$U_{i,G} = [U_{1i,G}, U_{2i,G}, \ldots, U_{ji,G}, \ldots, U_{Di,G}] \tag{8}$$

In DE algorithm, two kinds of crossover methods are used i.e. exponential and binomial (or uniform) (Price et al., 2005). In this work, binomial crossover strategy is used which can be described as:

$$U_{j,i,G} = \begin{cases} V_{j,i,G}, & \text{if } (rand \leqslant CR \text{ or } j = j_{rand}) \\ X_{j,i,G}, & \text{otherwise} \end{cases} \tag{9}$$

where CR is known as the crossover rate and appears as another control parameter of DE just like F. $j_{rand} \in [1, 2, \ldots, D]$ is a randomly chosen index, which ensures that $U_{i,G}$ attains at least one element from $V_{i,G}$.

A major problem in the conventional DE (Storn and Price, 1997) is the nonphysical values of the determined parameters (Michalewicz and Schoenauer, 1996). To avoid such situation, a penalty function is used. It ensures that the parameter values lie within the allowable range after recombination. Any parameter that violates the limits is replaced with random values using (Ishaque et al., 2011):

$$U_{i,G+1} = \begin{cases} U_{i,G+1} - rand[0,1](X_{iH} - X_{iL}) \text{ if } U_{i,G+1} > X_{iH} \\ U_{i,G+1} + rand[0,1](X_{iH} - X_{iL}) \text{ if } U_{i,G+1} < X_{iL} \end{cases} \tag{10}$$

3.4. Evaluation and selection

The selection operation at $G = G + 1$ is described

$$X_{i,G+1} = \begin{cases} U_{i,G} & \text{if } J(U_{i,G}) < J(X_{i,G}) \\ X_{i,G} & \text{otherwise} \end{cases} \tag{11}$$

where $J(X)$ is the objective function to be minimized. Thus, if the new trial vector acquires a lower value of the objective function, it swaps the corresponding target vector in the next generation; otherwise the target is preserved in the population. Hence, the population either gets better or remains the same in fitness status, but never declines. Fig. 5 shows the flow chart of DE process. The pseudo code of the proposed DE method is shown in Fig. 6.

4. Parameter determination of PV module using DE

Eq. (3) requires the computation of five parameters, namely I_{PV}, I_o, a, R_s, and R_p. In majority of the cases, the model incorporates merely the variations of photocurrent (I_{PV}) and diode saturation current (I_o), while the remaining parameters (a, R_s, and R_p) are kept constant or adjusted for better curve fitting (Walker, 2001). However, it is known that parameters of PV module are significantly affected by irradiance and temperature variations. Thus, for accurate modeling of a PV module, it is crucial to simultaneously compute all the five parameters at each environmental condition. In this work, we propose an optimization method to determine a, R_s, and R_p at operating points other than STC using differential evolution (DE) method. In contrast to other approach (Kim and Choi, 2010), which requires experimental $I-V$ data for every environmental condition, the proposed method only need STC information which are normally provided by the manufacturer's data sheet.

Fig. 7 shows a typical $I-V$ and $P-V$ curves. Usually, three points at STC (0, I_{sc}), (V_{mp}, I_{mp}) and (V_{oc}, 0) are available in datasheet. The goal of the modeling is to make accurate estimation of these points at irradiance and temperature other than STC.

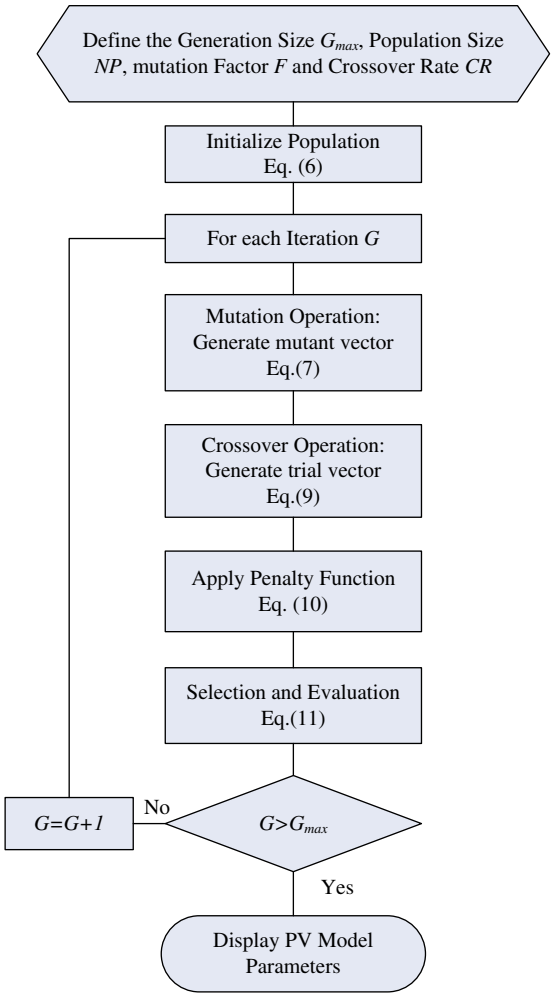

Fig. 5. Flow chart of DE.

The photo-current of the PV module as a function of solar irradiance and temperature variation can be written as (De Soto et al., 2006):

$$I_{PV} = (I_{PV\_STC} + K_I \Delta T)\frac{G}{G_{STC}} \tag{12}$$

where I_{PV_STC} (in Ampere) is the light generated current at STC, $\Delta T = T - T_{STC}$ (in Kelvin, $T_{STC\,=\,25\,^{\circ}C)}$, G is the surface irradiance of the cell and G_{STC} (1000 W/m^2) is the irradiance at STC.

For the R_p-model, an improved equation to describe the saturation current which considers the temperature variation is given by (Villalva et al., 2009), i.e.

$$I_o = \frac{I_{PV}}{\exp(V_{OC}/a/V_T) - 1} \tag{13}$$

where

$$V_{OC} = V_{OCn} + aV_T ln\left(\frac{G}{G_{STC}}\right) + K_V \Delta T \tag{14}$$

The equation at the M_{PP} can be written as:

Step 1
Setting values of the control parameters of DE:
Population size *NP*, crossover rate *CR*, mutation factor *F* and the Datasheet information of PV module.
Step 2
Set the generation number $G = 0$
and randomly initialize a population of *NP* individuals with $X_{i,G} = [X_{1,i,G}, X_{2,i,G}, X_{3,i,G}, ..., X_{D,i,G}]$ and each individual uniformly distributed in the range $[X_L, X_H]$ as:
$X_{j,I,0} = X_L + rand\,[0,1](X_H - X_L)$ where
$X_L = [X_{1,L}, X_{2,L}, ..., X_{D,L}]$ and
$X_H = [X_{1,H}, X_{2,H}, ..., X_{D,H}]$ with $i = [1, 2, ...,NP]$.
Step 3
WHILE the stopping criterion is not satisfied
DO
FOR i = 1 to *NP*
Step 3.1 Mutation Step
Generate a donor vector $V_{i,G} = [V_{1,i,G}, V_{2,i,G}, ..., V_{D,i,G}]$ corresponding to the i_{th} target vector $X_{i,G}$ using the differential mutation scheme of DE as:
$V_{i,G} = X_{r1,G} + F(X_{r2,G} - X_{r3,G})$
Step 3.2 Crossover Step
Generate a trial vector $U_{i,G} = [U_{1,i,G}, U_{1,i,G}, ..., U_{D,i,G}]$ for the i_{th} target vector $X_{i,G}$ through binomial crossover in the following way:
$U_{j,i,G} = V_{j,i,G}$, if $(rand_{i,j}[0, 1] \le CR$ or $j = j_{rand})$
$X_{j,i,G}$, otherwise,
Step 3.2.1 Penalty Function
IF $U_{j,i,G} < X_L$, THEN $U_{j,i,G} = X_L - rand\,[0,1](X_H - X_L)$
ELSEIF $U_{j,i,G} > X_H$, THEN $U_{j,i,G} = X_H - rand\,[0,1](X_H - X_L)$
END IF
Step 3.3 Selection and Evaluation Step
Evaluate the trial vector $U_{i,G}$
IF $J(U_{i,G}) < J(X_{i,G})$, THEN $X_{i,G+1} = U_{i,G}$
ELSE $X_{i,G+1} = X_{i,G}$.
END IF
END FOR
Step 3.4 Increase the Generation Count
$G = G + 1$
END WHILE

Fig. 6. Pseudo-code for the proposed DE algorithm.

$$V_{mp} = V_{mpn} + V_T ln\left(\frac{G}{G_{STC}}\right) + K_{VP}\Delta T \tag{15}$$

$$I_{mp} = I_{mpn}\left(\frac{G}{G_{STC}}\right)\{1 + K_{IP}\Delta T\} \tag{16}$$

Eqs. (12)–(16) represent the change in PV module parameters with respect to temperature and irradiance. The coefficients of temperature for current and voltage are usually provided in the manufacturer's data sheet. So, the changes in the values of I_{PV} and I_o can be obtained if the precise values of a, R_s, and R_p are known.

Like the other evolutionary algorithms, the optimization process in DE is based on the minimization/maximization

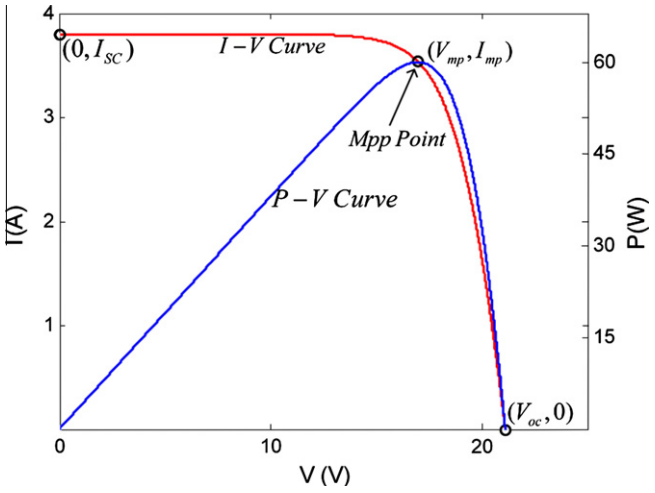

Fig. 7. I–V and P–V characteristic curve.

of an objective function. Therefore, a suitable objective function must be defined to begin the optimization process. Fig. 8a and b shows the typical $I-V$ and $P-V$ curves of a PV module, for different irradiance ($\lambda = 1$ is equivalent to 1000 W/m^2) and temperature levels, respectively.

It can be seen from Fig. 8, at M_{PP}, the derivative of the power with respect to voltage is zero (i.e. $\frac{dP}{dV} = 0$). According to the basic power equation:

$$P = VI \tag{17}$$

Taking the derivative of Eq. (16), it gives:

$$\frac{dP}{dV} = V\frac{dI}{dV} + I \tag{18}$$

Eq. (17) can serve as an objective function for the optimization problem, which in this case minimization of Eq. (17). Hence,

$$J = \left|\left.\frac{dI}{dV}\right|_{(V_{mp},I_{mp})} + \frac{I_{mp}}{V_{mp}}\right| \tag{19}$$

where $\frac{dI}{dV}$ can be obtained from Eq. (2) as:

$$\frac{dI}{dV}|\,(V_{mp}, I_{mp}) = -\frac{I_o\Gamma\exp\{\Gamma(V_{mp} + I_{mp}R_s)\} - G_p}{1 + I_o\Gamma R_s\exp\{\Gamma(V_{mp} + I_{mp}R_s)\} + G_pR_s} \tag{20}$$

and

$$\Gamma = \frac{1}{aV_T} \text{ and } G_p = \frac{1}{R_p} \tag{21}$$

Using Eq. (19) as the objective function, a search and optimization problem for determination of optimal values of a, R_s, and R_p can be defined. The PV module parameters can therefore be determined by the following process: given a set of data (from datasheet) of a particular PV module, the DE method is applied to update the parameters by minimizing of Eq. (19).

5. Results and discussion

The accuracy of modeling method described in this paper is validated by measured parameters of selected PV modules. The experimental (I, V) data is extracted from the manufacturer's datasheet (Shell, xxxx). Three modules of different technologies are utilized for verification; these include the multi- and mono-crystalline as well as thin-film types. The specifications of the modules are summarized in Table 1. The values for the temperature coefficients for power (K_{IP}, and K_{VP}) are taken from the Sandia National Laboratory (SNL) documents, which provide a list of these coefficients for the varieties of PV modules (King, 2000).

For the DE implementation, population size (NP) is chosen to be 30. This is a reasonable choice; typical values of NP ranged between $5D$ and $10D$. The maximum generation number ($G_{\max}$) is set to 100. The mutation scaling

Table 1
Specifications for the three modules used in the experiments.

Parameter	Mono-crystalline SM55	Multi-crystalline S75	Thin film ST40
I_{sc}	3.45	4.7	2.68
V_{oc}	21.7	21.6	23.3
I_{mp}	3.15	4.26	2.41
V_{mp}	17.4	17.6	16.6
K_v (m/°C)	76	76	100
K_i (m/°C)	1.4	0.45	0.35
K_{vp} (m/°C)	76	76	100
K_{ip} (m/°C)	0.14	0.14	0.45
N_s	36	36	42

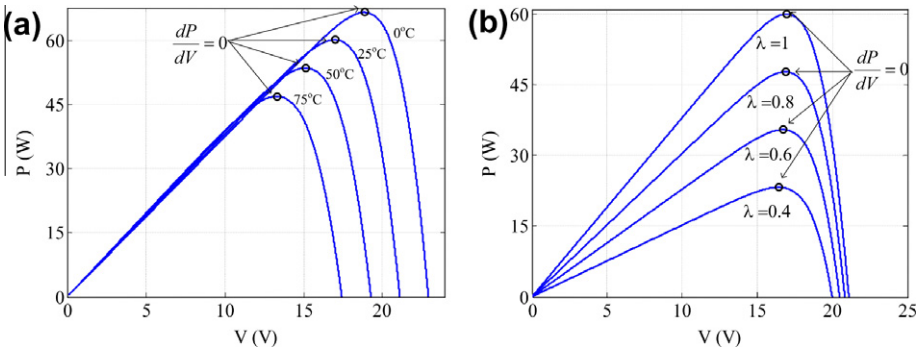

Fig. 8. PV curves (a) for irradiance variation (b) for temperature variation.

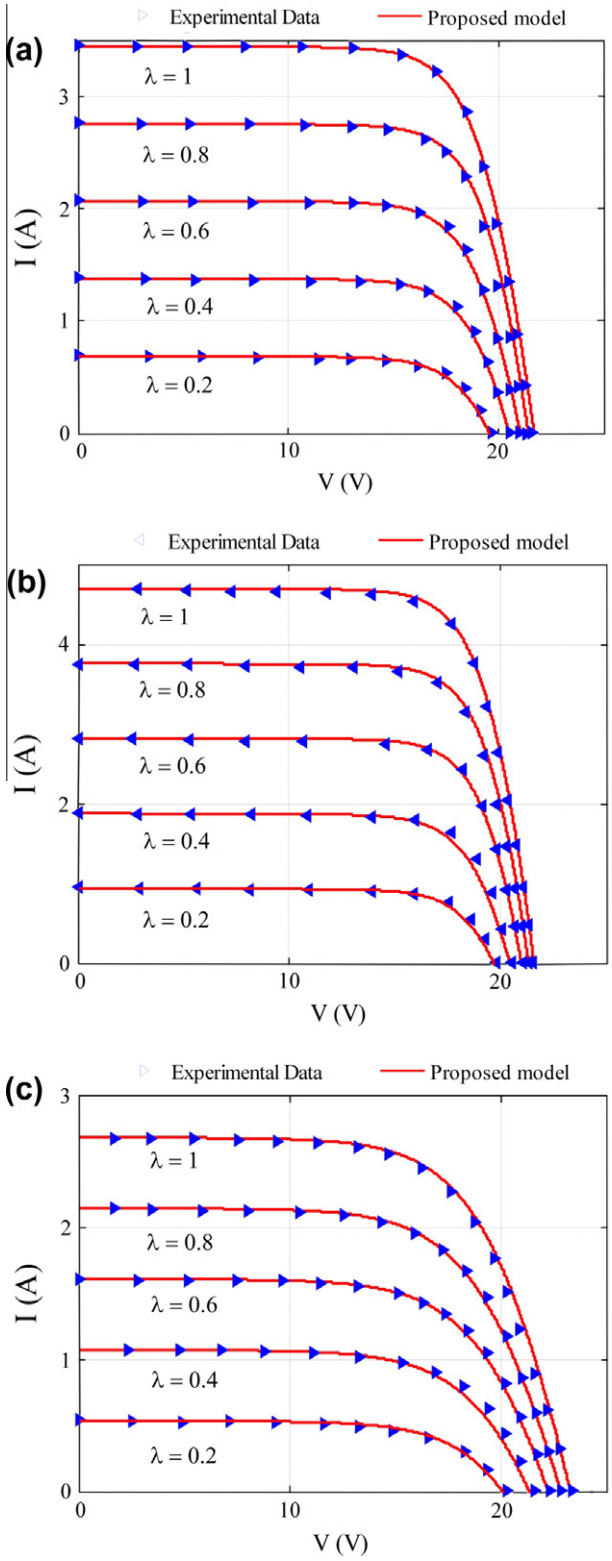

Fig. 9. $I-V$ curves for different irradiation levels (a) SM55 (mono-crystalline), (b) S75 (multi-crystalline) and (c) ST40 (thin film). *Note*: $\lambda = 1$ is equivalent to 1000 W/m^2.

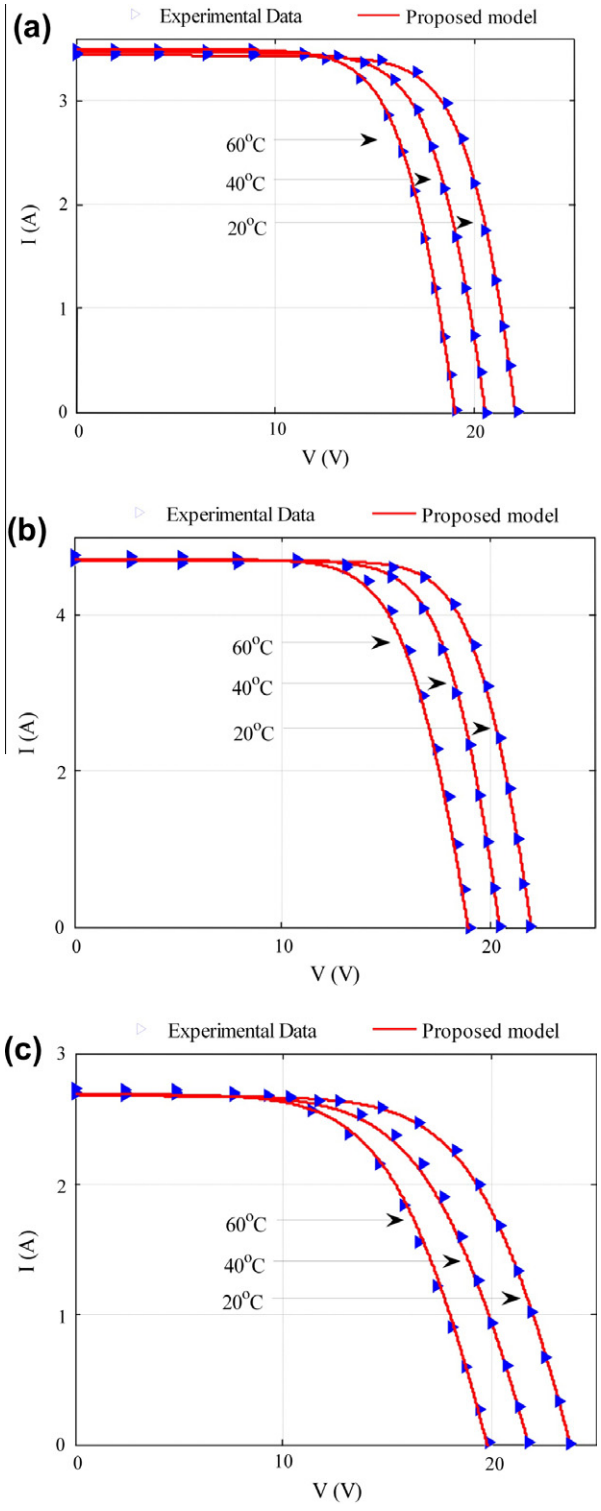

Fig. 10. The $I-V$ curves for different temperature levels (a) SM55 (mono-crystalline), (b) S75 (multi-crystalline) and (c) ST40 (thin film).

factor (F) is set at 0.4. The crossover rate (CR) is chosen to be 0.4. These values are adopted according to Priyanka et al. (2007). In PV module, usually, series resistance R_s is found to be very low, and most of the cases, less than 1Ω (Villalva et al., 2009). However, parallel resistance R_p value is very high. The value of ideality factor a is typically between $1 \leqslant a \leqslant 2$ (Villalva et al., 2009). In view of these data, the search ranges were set as follows: $R_s \in [0.1, 1]$,

Table 2
Parameters for the proposed model.

Parameter	Mono-crystalline SM55		Multi-crystalline S75		Thin film ST40	
	Proposed model	R_s-model	Proposed model	R_s-model	Proposed model	R_s-model
$G = 1000$ W/m^2						
a	1.37	1.3	1.33	1.3	1.97	1.2
R_s (Ω)	0.3	0.25	0.2	0.34	0.71	0.092
R_p (KΩ)	2.34	∞	1.79	∞	1.62	∞
$G = 800$ W/m^2						
a	1.34	1.3	1.28	1.3	2	1.2
R_s (Ω)	0.37	0.25	0.28	0.34	0.77	0.092
R_p (KΩ)	1.1	∞	0.798	∞	2.29	∞
$G = 600$ W/m^2						
a	1.1	1.3	1.44	1.3	1.83	1.2
R_s (Ω)	0.74	0.25	0.11	0.34	0.84	0.092
R_p (KΩ)	1.14	∞	1.27	∞	0.702	∞
$G = 400$ W/m^2						
a	1.43	1.3	1.28	1.3	1.81	1.2
R_s (Ω)	0.42	0.25	0.33	0.34	0.99	0.092
R_p (KΩ)	2.76	∞	1.4	∞	1.25	∞
$G = 200$ W/m^2						
a	1.34	1.3	1.24	1.3	1.73	1.2
R_s (Ω)	0.63	0.25	0.17	0.34	0.91	0.092
R_p (KΩ)	1.79	∞	1.45	∞	2.34	∞

Table 3
Parameters for the proposed model.

Parameter	Mono-crystalline SM55		Multi-crystalline S75		Thin film ST40	
	Proposed model	R_s-model	Proposed model	R_s-model	Proposed model	R_s-model
$T = 20$ °C						
a	1.47	1.2	1.54	1.2	1.96	1.2
R_s (Ω)	0.24	0.25	0.22	0.34	0.76	0.092
R_p (KΩ)	2.16	∞	0.887	∞	2.5	∞
$T = 40$ °C						
a	1.36	1.2	1.48	1.2	1.89	1.2
R_s (Ω)	0.3	0.25	0.17	0.34	0.8	0.092
R_p (KΩ)	2	∞	2.4	∞	1.64	∞
$T = 60$ °C						
a	1.35	1.2	1.39	1.2	1.7	1.2
R_s (Ω)	0.31	0.25	0.14	0.34	0.98	0.092
R_p (KΩ)	2.2	∞	640	∞	2.7	∞

$R_p \in [100, 3000]$, $a \in [1, 2]$. The DE/best/1/bin strategy is used in the proposed work. In this nomenclature, the word "best" defines the best vector from the current population, "1" specifies number of difference vector and "bin" describes the binomial crossover technique. Due to stochastic nature of the DE, the model is executed for 10 times and the resulting average values are taken as the model parameters.

Fig. 9a–c shows the I–V curves for SM55, S75 and ST40 respectively, for different levels of irradiance. It can be seen that the I–V curve obtained by proposed model strongly agrees to the experimental data for all types of modules. In particular, the proposed model is very accurate at low irradiance levels (Ishaque et al., 2011).

The I–V curves for the R_s-model (depicted in Fig. 2) are not shown for brevity. However a detailed comparison (in the form of errors) between the proposed and R_s-model will be undertaken in the next subsection.

The performance of the proposed model when subjected to temperature variation is shown in Fig. 10a–c. The accuracy of the model was tested at 20°, 40° and 60 °C. All measurements are performed at STC irradiance of 1000 W/m^2. It can be observed that the I–V curve of the proposed model matches accurately to the experimental data for all three temperature conditions.

To quantify the accuracy of the proposed method, results are compared to the R_s-model. Table 2 lists the model parameters values computed using the proposed

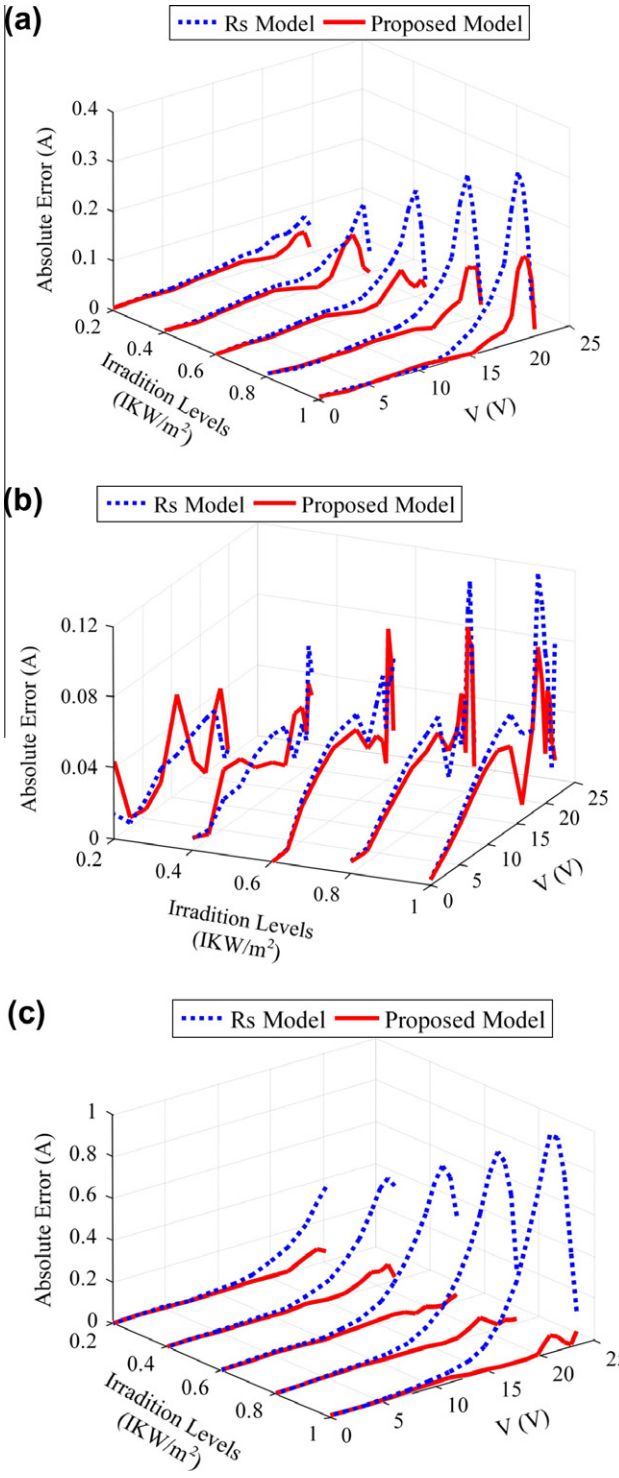

Fig. 11. Absolute errors for different irradiation levels (a) SM55 (mono-crystalline), (b) S75 (multi-crystalline) and (c) ST40 (thin film).

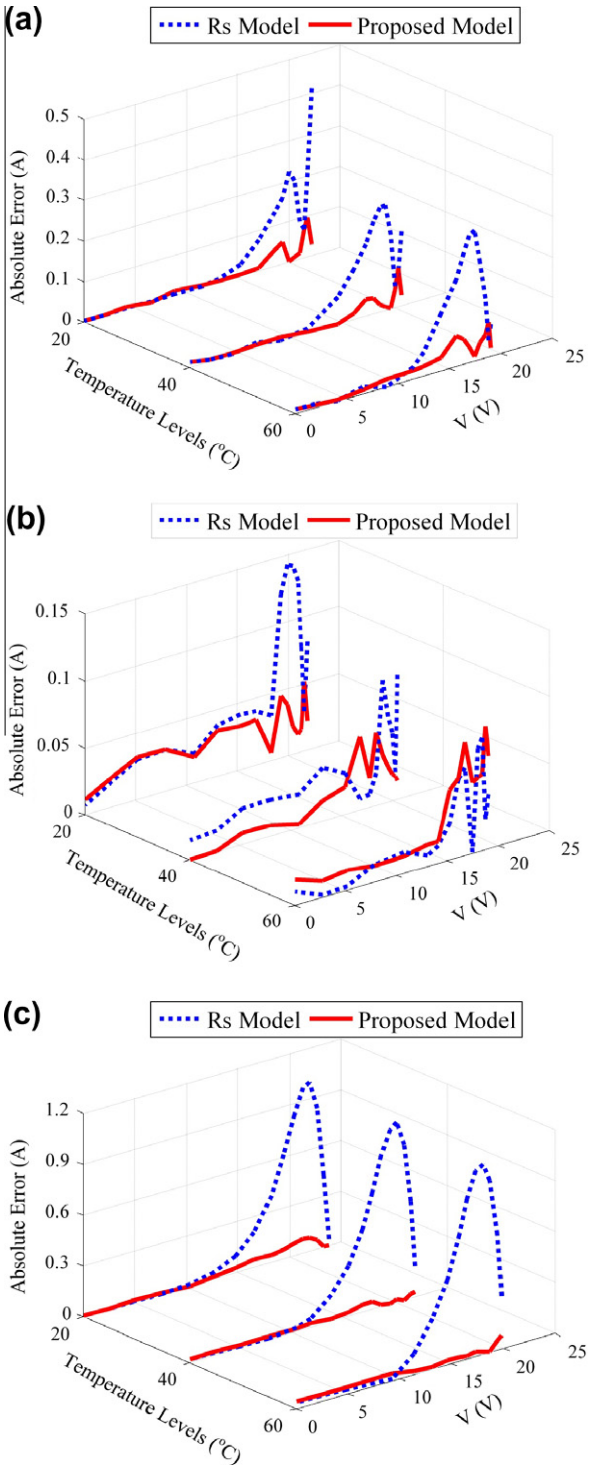

Fig. 12. Absolute errors for different temperature levels (a) SM55 (mono-crystalline), (b) S75 (multi-crystalline) and (c) ST40 (thin film).

and R_s-model for irradiance variations. It can be seen, using R_s-model, the same values of a, R_s and R_p are obtained regardless of the irradiance. This is to be expected because the model does not consider the environmental variations in the formulation of its equations. However for the proposed method, the parameters values do vary for different irradiance levels. Logically this can be considered more accurate because it takes it to account the slope variation at V_{oc} of the $I-V$ curves. These observations are also consistent with (Priyanka et al., 2007; Singh et al., 2008; Khan et al., 2010).

For the thin-film module, marked differences are noticed between the proposed and R_s-model. The value of series resistance is constant and approximately one order of magnitude less for the former for all irradiance levels. Such small value is not appropriate for thin film module (Deb and Ghosh, 1984; Stutenbaeumer and Mesfin, 1999). The value of series resistance computed using the proposed model is more realistic and is in close agreement with results published elsewhere (Guimard et al., 2002). Furthermore, small value of a is obtained using the R_s-model. This value is not accurate, because for thin film, the small fill factor should result in large values of a (Sites and Mauk, 1989; Kassis and Saad, 2003).

The computed parameters using the proposed model and R_s-model for temperature variations are listed in Table 3. For the case of R_s-model i.e. same values of a, R_s and R_p are obtained which is not accurate if temperature variations is considered. For the proposed model, the ideality factor, a, decreases with temperature, which agrees with the work reported in (Sites and Mauk, 1989; Sharma et al., 1990). Similar results are obtained for the thin-film module. For the series resistance using R_s-model, one order of magnitude difference is observed for all values of temperature. Likewise, a noticeably large values of a is obtained using the proposed model which is again in close agreement to the one calculated by Sandia model (King, 2000).

For a comprehensive comparison, the errors between the proposed and R_s-model are computed. The absolute error is defined as the absolute difference between the experimental and computed current values of the $I-V$ curves for a given voltage point. These are carried out for various irradiance and temperature levels as shown in Fig. 11a–c to Fig. 12a–c, respectively.

In general, the proposed model exhibits lower errors for all environmental conditions. In most cases, the maximum errors occur near the vicinity of MPP. This is to be expected because the value of the series resistance plays a dominant role in determining the curvature of the $I-V$ curve. The curvature is the region where the MPP lies. For the R_s-model, the value of series resistance is constant for all environmental conditions as shown in Table 2 and 3. When the irradiance or temperature varies, this fixed value of R_s will result in inaccurate $I-V$ curve at this region. On the other hand, for the proposed model, the series resistance value changes with the environmental conditions. This means that for every irradiance and temperature value, the R_s is appropriately computed. That explains why the error is reduced.

In the particular case of thin film module, the error for R_s-model is exceptionally high. This can be attributed to the fact that R_s is very low – as explained earlier by Tables 2 and 3. Although the value of R_s can be increased by increasing the ideality factor a, the result is counterproductive. It was found that if large a is used (for example $a > 1.5$) negative value of R_s is obtained. This is a non-physical value and must be omitted.

6. Conclusion

In this paper, a differential evolution (DE) based modeling method for PV module is described. Unlike the previous models suggested by other researchers, the proposed work computes the PV module parameters at any irradiance and temperature point, using only the datasheet information for a PV module. The accuracy of the proposed model is evaluated using experimental data from the manufacturers of three PV modules of different types. Its performance is compared to the popular single diode R_s-model. It was found that in all cases, the proposed model is superior when subjected to irradiance and temperature variations. It is envisaged that the proposed model can be a valuable design tool for PV system designers.

Acknowledgments

The authors would like to thank Universiti Teknologi Malaysia for providing the facilities and research grant to conduct this research.

References

Almonacid, F., Rus, C., et al., 2009. Characterisation of Si-crystalline PV modules by artificial neural networks. Renewable Energy 34 (4), 941–949.

Almonacid, F., Rus, C., et al., 2010. Characterisation of PV CIS module by artificial neural networks. A comparative study with other methods. Renewable Energy 35 (5), 973–980.

Balzani, M., Reatti, A., 2005. Neural network based model of a PV array for the optimum performance of PV system. Research in Microelectronics and Electronics, 2005 PhD.

Carrero, C., Amador, J., et al., 2007. A single procedure for helping PV designers to select silicon PV modules and evaluate the loss resistances. Renewable Energy 32 (15), 2579–2589.

Chegaar, M., Ouennoughi, Z., et al., 2001. A new method for evaluating illuminated solar cell parameters. Solid-State Electronics 45 (2), 293–296.

Chenni, R., Makhlouf, M., et al., 2007. A detailed modeling method for photovoltaic cells. Energy 32 (9), 1724–1730.

De Soto, W., Klein, S.A., et al., 2006. Improvement and validation of a model for photovoltaic array performance. Solar Energy 80 (1), 78–88.

Deb, S., Ghosh, B., 1984. Series resistance and optimum grid design for a thin film solar cell of rectangular shape. Solar Cells 13 (2), 145–162.

Elshatter, T. F., M. E. Elhagree, et al. (1997). Fuzzy Modeling and Simulation of Photovoltaic. In: 14th European Photovoltaic Solar Energy Conference. Spain.

Gow, J.A., Manning, C.D., 1999. Development of a photovoltaic array model for use in power-electronics simulation studies. IEE Proceedings – Electric Power Applications 146 (2), 193–200.

Guimard, D., Grand, P.P., et al., 2002. Copper indium diselenide solar cells prepared by electrodeposition. In: Photovoltaic Specialists Conference, 2002. Conference Record of the Twenty-Ninth IEEE.

Ishaque, K., Salam, Z., et al., 2011. Simple, fast and accurate two-diode model for photovoltaic modules. Solar Energy Materials and Solar Cells 95 (2), 586–594.

Ishaque, K., Salam, Z., et al., 2011. A critical evaluation of EA computational methods for Photovoltaic cell parameter extraction based on two diode model. Solar Energy 85 (9), 1768–1779.

Jervase, J.A. et al., 2001. Solar cell parameter extraction using genetic algorithms. Measurement Science and Technology 12 (11), 1922.

Ji, M., Jin, Z., et al., 2006. An improved simulated annealing for solving the linear constrained optimization problems. Applied Mathematics and Computation 183 (1), 251–259.

Kajihara, A., Harakawa, A.T., 2005. Model of photovoltaic cell circuits under partial shading. In: IEEE International Conference on Industrial Technology, 2005. ICIT 2005.

Karatepe, E., Boztepe, M., et al., 2006. Neural network based solar cell model. Energy Conversion and Management 47 (9–10), 1159–1178.

Kassis, A., Saad, M., 2003. Fill factor losses in ZnO/CdS/CuGaSe2 single-crystal solar cells. Solar Energy Materials and Solar Cells 80 (4), 491–499.

Kassis, A., Saad, M., 2010. Analysis of multi-crystalline silicon solar cells at low illumination levels using a modified two-diode model. Solar Energy Materials and Solar Cells 94 (12), 2108–2112.

Khan, F., Singh, S.N., et al., 2010. Effect of illumination intensity on cell parameters of a silicon solar cell. Solar Energy Materials and Solar Cells 94 (9), 1473–1476.

Khouzam, K., L. Cuong, et al. (1994). Simulation and real-time modelling of space photovoltaic systems. In: 1994 IEEE First World Conference on Photovoltaic Energy Conversion, 1994. Conference Record of the Twenty Fourth. IEEE Photovoltaic Specialists Conference – 1994.

Kim, W., Choi, W., 2010. A novel parameter extraction method for the one-diode solar cell model. Solar Energy 84 (6), 1008–1019.

King, D.L., Sandia's PV Module Electrical Performance Model (Version, 2000), September 5.

Matagne, E., Chenni, R., et al., 2007. A photovoltaic cell model based on nominal data only. In: 2007 International Conference on Power Engineering, Energy and Electrical Drives POWERENG 2007.

Mellit, A., Benghanem, M., et al., 2007. Modeling and simulation of a stand-alone photovoltaic system using an adaptive artificial neural network: proposition for a new sizing procedure. Renewable Energy 32 (2), 285–313.

Michalewicz, Z., Schoenauer, M., 1996. Evolutionary algorithms for constrained parameter optimization problems. Evolutionary Computation 4 (1), 1–32.

Moldovan, N., Picos, R., et al., 2009. Parameter extraction of a solar cell compact model usign genetic algorithms. In: Spanish Conference on Electron Devices 2009. CDE 2009.

Nishioka, K., Sakitani, N., et al., 2007. Analysis of multicrystalline silicon solar cells by modified 3-diode equivalent circuit model taking leakage current through periphery into consideration. Solar Energy Materials and Solar Cells 91 (13), 1222–1227.

Price, K.V., Storn, R.M., et al., 2005. Differential Evolution A Practical Approach to Global Optimization. Springer.

Priyanka, Lal, M., et al., 2007. A new method of determination of series and shunt resistances of silicon solar cells. Solar Energy Materials and Solar Cells 91 (2–3), 137–142.

Sera, D., Teodorescu, R., et al., 2007. PV panel model based on datasheet values. In: IEEE International Symposium on Industrial Electronics, 2007. ISIE 2007.

Sharma, S.K. et al., 1990. Overcoming the problems in determination of solar cell series resistance and diode factor. Journal of Physics D: Applied Physics 23 (9), 1256.

Shell, Shell Solar Product Information Sheet. <http://www.solarcell-sales.com/techinfo/technical_docs.cfm>.

Shengyi, L., Dougal, R.A., 2002. Dynamic multiphysics model for solar array. IEEE Transactions on Energy Conversion 17 (2), 285–294.

Singh, P., Singh, S.N., et al., 2008. Temperature dependence of *I–V* characteristics and performance parameters of silicon solar cell. Solar Energy Materials and Solar Cells 92 (12), 1611–1616.

Sites, J.R., Mauk, P.H., 1989. Diode quality factor determination for thin-film solar cells. Solar cells 27 (1–4), 411–417.

Storn, R., Price, K., 1997. Differential evolution – a simple and efficient heuristic for global optimization over continuous spaces. Journal of Global Optimization 11 (4), 341–359.

Stutenbaeumer, U., Mesfin, B., 1999. Equivalent model of monocrystalline, polycrystalline and amorphous silicon solar cells. Renewable Energy 18 (4), 501–512.

Syafaruddin, Karatepe, E., et al., 2010. Development of Real-Time Simulator Based on Intelligent Techniques for Maximum Power Point Controller of Photovoltaic System, vol. 6(4), p. 20.

Villalva, M.G., Gazoli, J.R., et al., 2009. Comprehensive approach to modeling and simulation of photovoltaic arrays. IEEE Transactions on Power Electronics 24 (5), 1198–1208.

Walker, G., 2001. Evaluating MPPT converter topologies using a MATLAB PV model. Journal of Electrical & Electronics Engineering Australia 21 (1), 8.

Weidong, X., Dunford, W.G., et al., 2004. A novel modeling method for photovoltaic cells. In: 2004 IEEE 35th Annual Power Electronics Specialists Conference, 2004. PESC 04.

Ye, M., Wang, X., et al., 2009. Parameter extraction of solar cells using particle swarm optimization. Journal of Applied Physics 105 (9), 094502–094508.

Yun Tiam, T., Kirschen, D.S., et al., 2004. A model of PV generation suitable for stability analysis. IEEE Transactions on Energy Conversion 19 (4), 748–755.

Zwe-Lee, G., 2004. A particle swarm optimization approach for optimum design of PID controller in AVR system. IEEE Transactions on Energy Conversion 19 (2), 384–391.